Complementary bowtie aperture for localizing and enhancing optical magnetic field

Nan Zhou,† Edward C. Kinzel,† and Xianfan Xu*

School of Mechanical Engineering and Birck Nanotechnology Center, Purdue University, West Lafayette, Indiana 47907, USA

**Corresponding author: xxu@purdue.edu*

Received May 11, 2011; revised June 21, 2011; accepted June 22, 2011; posted June 24, 2011 (Doc. ID 147305); published July 19, 2011

Nanoscale bowtie antenna and bowtie aperture antenna have been shown to generate strongly enhanced and localized electric fields below the diffraction limit in the optical frequency range. According to Babinet's principle, their complements will be efficient for concentrating and enhancing magnetic fields. In this Letter, we discuss the enhancement of magnetic field intensity of nanoscale complementary bowtie aperture as well as complementary bowtie aperture antenna, or diabolo nanoantenna. We show that the complementary bowtie antenna resonates at a smaller wavelength and thus is more suitable for applications near visible wavelengths. The near-field magnetic intensity can be further enhanced by the addition of groove structures that scatter surface plasmon.

OCIS codes: 240.0240, 050.1220, 240.6680.

Babinet's principle is a classical theory in optics [1]. It states that for an infinitely thin, perfectly conducting plane, a similar response can be anticipated if a complementary structure is illuminated with a complementary wave. An extension of it was introduced to include the polarization effect [2]. Recently, Babinet's principle has been applied as an approximation for metamaterials with a finite thickness [3]. An important recent development in nano-optics is nanoantenna, which can localize and enhance the electric field. Nanoscale bowtie antenna (BA) [4–6] and bowtie aperture antenna (BAA) [7–9] are two examples. On the other hand, it is also desirable to obtain strongly localized and enhanced magnetic field. Indeed, a recent work showed that by applying Babinet's principle, magnetic field confinement and enhancement could be achieved in near-IR by using the complement of a BAA called diabolo antenna (DA) [10]. Figure 1 shows the geometry and relationship among the four bowtie-related structures. For electrical field enhancement in BA and BAA, when excited with correct polarization (indicated as black arrows in the figure), charges accumulate at the apexes of the two metal triangles, which cause a large electric field in the gap. For DA and complementary bowtie aperture (CBA), the current along the metal strip leads to a large magnetic field around the metal strip. In this Letter, we numerically investigate CBA and DA for localizing and enhancing magnetic field in the optical and near-IR frequencies. We also investigate means to further increase the magnetic field enhancement. It is noted that there are methods other than Babinet's principle for studying the electric and magnetic enhancement, one of which is the use of charge and current reservoirs [11].

A finite-element frequency-domain method [12], same as used in the study of BA and BAA [13], is employed to study CBA and DA. The model uses gold film deposited on a glass substrate (with an index of refractive of 1.5), and surrounded by air, as shown in the insert of Fig. 1(d). Optical properties are taken from [14]. The symbols a and d in Fig. 1(d) define the width of the entire structure and the width of the central strip. The flare angles are fixed at 45°. CBA or DA is illuminated by a plane wave from the substrate side at normal incidence and polarized along the x direction. The length a is varied, where d and the film thickness t are fixed at 20 nm. It was reported that for DA, smaller d and t produce larger enhancement [10]. We choose the same d and t values as in [10], and our results (not shown here) did confirm that larger d and t would reduce magnetic enhancement. We normalize intensities generated by nanostructures to those without the presence of such metal films, and define them as the intensity enhancement.

Figure 2 shows magnetic responses of CBA and DA with various lengths a. Note the different intensity scales for large (in blue) and short lengths (in black). The resonances are related to charge oscillations along the metal strip and thus can be interpreted as plasmonic resonances [15]. The lowest order resonance is the strongest, whereas higher orders provide minimal enhancement and are not discussed here. Figure 2 shows that a size 620 nm CBA and a 260 nm DA have an enhancement maximum at the same wavelength of 2150 nm, a 310 nm CBA and a 135 nm DA have an enhancement maximum at 1400 nm, and a 150 nm CBA and a 52 nm DA have an enhancement maximum at 800 nm. Several trends can be noted from Fig. 2: larger CBA has the same resonance wavelength as smaller DA, larger CBA/DA has a longer resonance wavelength, and DA has a higher enhancement than CBA. These will be further discussed below.

To illustrate plasmonic resonance, Figs. 3(a) and 3(b) show the volume current density of a 620 nm CBA at

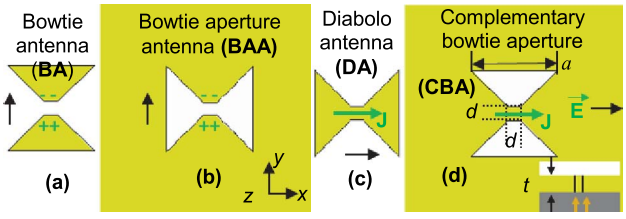

Fig. 1. (Color online) Geometry and relationship among the four bowtie-related structures: (a) bowtie antenna (BA) (b) bowtie aperture antenna (BAA) (c) diabolo antenna (DA) (d) complementary bowtie aperture (CBA).

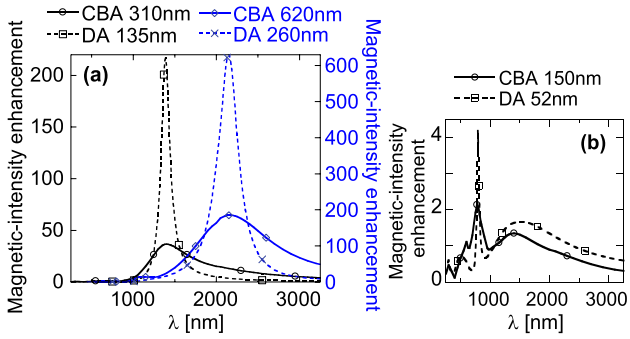

Fig. 2. (Color online) Magnetic spectral responses of CBA and DA with various lengths: (a) a 310 nm CBA and a 135 nm DA (in black), a 620 nm CBA and a 260 nm DA (in blue); (b) a 150 nm CBA and a 52 nm DA. All cases are calculated at a point in air that is 10 nm from the center of the exit plane of the metal strip.

wavelengths of 2150 nm (resonance) and 1500 nm (off-resonance). It can be seen from Fig. 3(a) that at resonance, the current densities in the central strip and around the structure are generally along the same direction. The current is drawn from all the metal surfaces and funneled toward the center strip. Hence, a larger dimension creates a higher enhancement as seen in Fig. 2. At off-resonance shown in Fig. 3(b), the current density is canceled out near the center of the metal strip, which leads to a small enhancement (the current at the center points to the right, and the majority of the rest of the current points to the left).

Different sizes of CBA and DA resonating at the same wavelength can also be understood by comparing the volume current densities (Figs. 3(a) and 3(c)). In CBA, the metal surrounding the aperture produces current density in phase with the central current density at resonance. However, around the corners (the right corners in Fig. 3(a)), the two current densities meet with opposite directions and thus weaken the funnel effect. This weakening occurs in the left corners when the current flows in the opposite direction. Hence, the effective length of

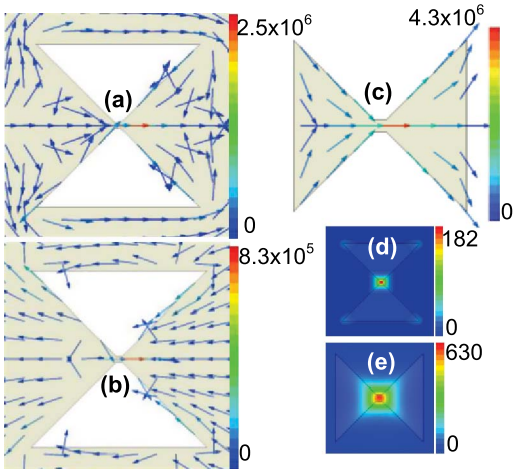

Fig. 3. (Color online) Volume current densities in the middle plane of the film for a 620 nm CBA at (a) 2150 nm, (b) 1500 nm, and (c) for a 260 nm DA at 2150 nm. (d), (e) Corresponding normalized magnetic intensity distributions for (a, c) in the xy plane in air (10 nm from the exit plane of the aperture). The incident field is specified with $E = 1\,\mathrm{V/m}$. The unit of the volume current density is $\mathrm{A/m^2}$.

CBA is reduced. For DA, the current density does not flow around the metal corners, and, therefore, does not reduce the current density at the center metal strip. Overall, two effects are produced: (1) the effective length of CBA is shorter compared with DA. This is shown in Fig. 2 that for a given resonance wavelength, the dimension of CBA is more than twice the dimension of DA. (2) At the same resonance frequency, CBA produces a lower magnetic field enhancement compared with DA.

The magnetic spot sizes produced by CBA and DA, shown in Figs. 3(d) and 3(e), are similar. CBA produces a full-width at half-maximum (FWHM) size of $59.5\,\mathrm{nm}(x) \times 46.7\,\mathrm{nm}(y)$, which is determined by the width of the central strip, and DA has a FWHM of $47\,\mathrm{nm}(x) \times 60\,\mathrm{nm}(y)$. The sizes of the magnetic spots at other resonance wavelengths are all similar, about $50\,\mathrm{nm}(x) \times 40\,\mathrm{nm}(y)$ for CBA and $40\,\mathrm{nm}(x) \times 50\,\mathrm{nm}(y\,\mathrm{nm})$ for DA.

Since CBA generates a magnetic spot at a smaller wavelength than DA, it is more promising to be used at shorter wavelengths. However, at shorter wavelengths, both structures produce a low magnetic enhancement. As shown in Fig. 2(b), at 800 nm, DA has a resonant dimension of only about 52 nm, making it difficult to be fabricated practically, whereas the resonant dimension is 150 nm for CBA. However, this 150 nm CBA has an enhancement of only about 2.1. A strategy to increase the enhancement is to place periodic grooves surrounding the aperture [16–19]. (Clearly, these grooves can only be added to CBA). Figure 4(a) shows that grooves are defined by width w_n, periodicity p, depth, and position of the first groove r_1. Since the current density along the metal strip needs to be increased, the grooves need to be placed only along the polarization axis as shown in Fig. 4(a). The depth of the groove is fixed as half of the film thickness t. With the addition of the grooves, the enhancement of the magnetic field is increased, and this enhancement increases with the number of grooves as seen in Fig. 4(b). The inset in Fig. 4(b) shows that the enhancement saturates at six grooves, similar to the results in [18,20], which were aiming at increasing optical transmission in a bull's eye structure. In our case, the six-groove structure leads to a magnetic intensity enhancement of about 70, or a relative enhancement compared to a structure without grooves of $70/2.1 = 33.3$.

The dimensions of the grooves described above have been chosen to maximize the magnetic intensity

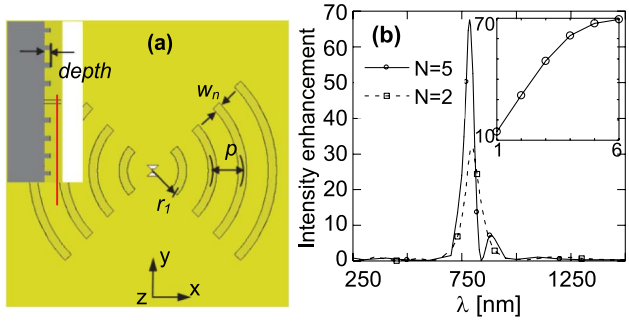

Fig. 4. (Color online) (a) Geometry of CBA with grooves. $d = t = 20\,\mathrm{nm}$ and $a = 150\,\mathrm{nm}$. (b) Magnetic responses of two- and five-groove structures. $r_1 = 348\,\mathrm{nm}$, $w_n = 117\,\mathrm{nm}$, $p = 385\,\mathrm{nm}$. Inset of (b) the maximum enhancement as a function of the number of grooves.

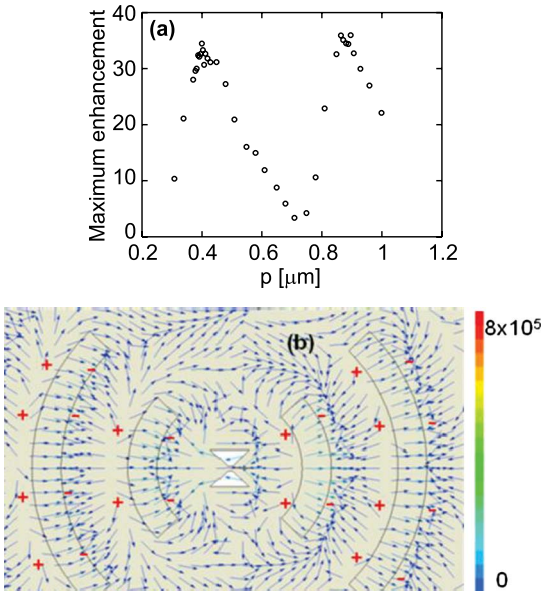

Fig. 5. (Color online) (a) Maximum intensity enhancement as a function of p for the two-groove structure. (b) Volume current density for two-groove structure at 800 nm.

enhancement at 800 nm wavelength. The periodicity p is most influential in the resulting magnetic field. This is illustrated in Fig. 5(a), which shows the maximum intensity enhancement as a function of p for a two-groove structure. When p equals 385 nm and 880 nm, significant enhancement is observed, and their difference is about 495 nm, close to the surface plasmon wavelength 508 nm for the Au/glass interface at 800 nm. Figure 5(b) shows the vectorial map of the volume current density on an x-y plane in gold, which is 5 nm above the grooves (shown as the red line in Fig. 4(a)). For plasmon interactions with periodic grooves, charges accumulate near the edges of the grooves [21], which are also seen in Fig. 5(b). These charges drive oscillating currents, shown as the currents in the direction "across" the grooves. It is seen that the grooves funnel the current toward the center, hence enhancing the magnetic field.

In summary, this work demonstrates that strongly enhanced and localized magnetic field can be generated with CBA and DA. In CBA, the metal surrounding the aperture triangles weakens the current funnel effect in the metal arms, leading to a smaller enhancement compared with DA. While in the near visible range, CBA is more promising to be used due to its relatively large dimension. Its magnetic field enhancement can be further increased with the use of periodic grooves.

The authors gratefully acknowledge the support of the National Science Foundation (NSF), Grant No. DMI-0707817; the Defense Advanced Research Projects Agency (DARPA), Grant No. N66001-08-1-2037; and the Air Force Office of Scientific Research (USAFOSR)-Multidisciplinary University Research Initiative program, Grant No. FA9550-08-1-0379.

[†]These authors contributed equally to this work.

References

1. M. Born and E. Wolf, *Principles of Optics*, 7th ed. (Cambridge University, 2002).
2. H. G. Booker, J. Inst. Elect. Eng. Part III A **93**, 620 (1946).
3. T. Zentgraf, C. Rockstuhl, T. P. Meyrath, A. Seidel, S. Kaiser, F. Lederer, and H. Giessen, Phys. Rev. B **76**, 033407 (2007).
4. R. D. Grober, R. J. Schoelkopf, and D. E. Prober, Appl. Phys. Lett. **70**, 1354 (1997).
5. P. J. Schuck, D. P. Fromm, A. Sundaramurthy, G. S. Kino, and W. E. Moerner, Phys. Rev. Lett. **94**, 017402 (2005).
6. N. Yu, E. Cubukcu, L. Diehl, D. Bour, S. Corzine, J. Zhu, G. Hofler, K. B. Crozier, and F. Capasso, Opt. Express **15**, 13272 (2007).
7. E. X. Jin and X. Xu, J. Quant. Spectrosc. Radiat. Transfer **93**, 163 (2005).
8. E. X. Jin and X. Xu, Appl. Phys. B **84**, 3 (2006).
9. E. X. Jin and X. Xu, Appl. Phys. Lett. **88**, 153110 (2006).
10. T. Grosjean, M. Mivelle, F. I. Baida, G. W. Burr, and U. C. Fischer, Nano Lett. **11**, 1009 (2011).
11. D. Wang, T. Yang, and K. B. Crozier, Opt. Express **18**, 10388 (2010).
12. HFSS 12.1, Ansoft LLC (2009).
13. E. C. Kinzel and X. Xu, Opt. Lett. **35** (7), 992 (2010).
14. E. D. Palik, *Handbook of Optical Constants of Solids* (Academic, 1998).
15. C. Rockstuhl, T. Zentgraf, C. Etrich, J. Kuhl, F. Lederer, and H. Giessen, Opt. Express **14**, 8827 (2006).
16. T. W. Ebbesen, H. J. Lezec, H. F. Ghaemi, T. Thio, and P. A. Wolff, Nature **391**, 667 (1998).
17. H. J. Lezec, A. Degiron, E. Devaux, R. A. Linke, L. Martin-Moreno, F. J. Garcia-Vidal, and T. W. Ebbesen, Science **297**, 820 (2002).
18. E. C. Kinzel, P. Srisungsitthisunti, Y. Li, A. Raman, and X. Xu, Appl. Phys. Lett. **96**, 211116 (2010).
19. D. Wang, T. Yang, and K. B. Crozier, Opt. Express **19**, 2148 (2011).
20. O. Mahboub, S. C. Palacios, C. Genet, F. J. Garcia-Vidal, S. G. Rodrigo, L. Martin-Moreno, and T. W. Ebbesen, Opt. Express **18**, 11292 (2010).
21. T. Thio, K. M. Pellerin, R. A. Linke, H. J. Lezec, and T. W. Ebbesen, Opt. Lett. **26** (24), 1972 (2001).